PHYSICAL REVIEW B **79**, 140101(R) (2009)

Theory of the mechanisms of pressure-induced phase transitions in oxygen

Hannelore Katzke[1,*] and Pierre Tolédano[2]
[1]*Institute of Geosciences, Crystallography, University of Kiel, Olshausenstraße 40, 24098 Kiel, Germany*
[2]*Laboratory of Physics of Complex Systems, University of Picardie, 33 rue Saint-Leu, 80000 Amiens, France*
(Received 2 February 2009; published 15 April 2009)

A theoretical description is proposed for the transition mechanisms relating the different phases of oxygen. In contrast to the current view, the antiferromagnetic order existing in the α and δ phases is shown to be structurally driven by the spontaneous deformations taking place at the $\beta \rightarrow \alpha$ and $\beta \rightarrow \delta$ transitions. The structural mechanism giving rise to $(O_2)_4$ clusters in the high-pressure ϵ phase is described and shown to be correlated with the magnetic collapse occurring at the $\delta \rightarrow \epsilon$ transition. The large intermediate region of coexistence between the ϵ and yet unknown higher-pressure ζ structures is suggested to correspond to a low-symmetry ferroelastic phase.

DOI: 10.1103/PhysRevB.79.140101 PACS number(s): 64.70.kt, 62.50.−p

Different types of structural transition mechanisms are involved in the phase diagram of solid oxygen. Below 8 GPa, one finds the reconstructive $\gamma \rightarrow \beta$ transition, which exhibits large displacements and orientational ordering of the molecules, and the magnetostructural $\beta \rightarrow \alpha$ and $\beta \rightarrow \delta$ transitions,[1,2] where small deformations are assumed to be induced by the magnetic ordering.[3–5] Further compression leads to the ϵ phase across a remarkable type of transition characterized by a magnetic collapse and the formation of molecular clusters containing four O_2 molecules.[6,7] At 96 GPa, the ϵ phase transforms progressively into the ζ phase,[8–10] corresponding to a profound modification of the electronic structure, giving rise to metallization in the absence of molecular-to-atomic dissociation. Because of the diversity of transition mechanisms between the phases of oxygen, there has been no attempt to give a unifying theoretical description of its phase diagram. Here, we propose a comprehensive picture of the transition mechanisms occurring in oxygen. In contrast with the current view, the antiferromagnetic order observed in α and δ-O_2 is interpreted as *structurally driven*. The magnetic collapse occurring at the $\delta \rightarrow \epsilon$ transition and the correlated structural mechanism inducing the formation of $(O_2)_4$ clusters in the ϵ structure are described.

The relationship between oxygen structures assumed in our description and the phase diagram of oxygen are shown in Fig. 1. The structures of five solid phases, namely α, β, γ, δ, and ϵ, are presently known. The cubic γ phase occupies a narrow range of temperature confined between the melting curve and the β phase. Figure 2(a) shows the large molecular displacements transforming the ordered β structure into the disordered γ structure [Fig. 2(b)]. The corresponding reconstructive transition mechanism can be described as proceeding via a rhombohedral shear-deformed γ structure shown in Fig. 2, displaying an eightfold β unit cell, induced by an instability at the L-point $(0, 2\pi/a, \pi/3c)$ of the rhombohedral Brillouin zone.[11]

The structural mechanism transforming β-O_2 into α-O_2 is shown in Fig. 3. It consists of antiparallel displacements of about 0.1 Å along the $[2\bar{2}1]$ hexagonal direction, corresponding to a shear strain e_{xz} which reduces the monoclinic β angle from 133.96° in β-O_2 to 132.53° in α-O_2. The $\beta \rightarrow \delta$ transition mechanism involves displacements of the same amount along $[210]_\beta$, reorienting the O_2 molecules along the $[212]_\beta$ direction (Fig. 3). Since the δ structure is not group subgroup related to β-O_2, the transition can be described as occurring via an intermediate common monoclinic substructure (Fig. 3), having the same structure as α-O_2 but a different orientation with respect to β-O_2; the δ structure resulting from a shearing of the α monoclinic structure.

Theoretical[12,13] and experimental studies[4,5,14] suggest that the $\beta \rightarrow \alpha$ and $\beta \rightarrow \delta$ structural transitions are magnetically driven. This interpretation can be tested by considering the *effective* free energy associated with the magnetostructural

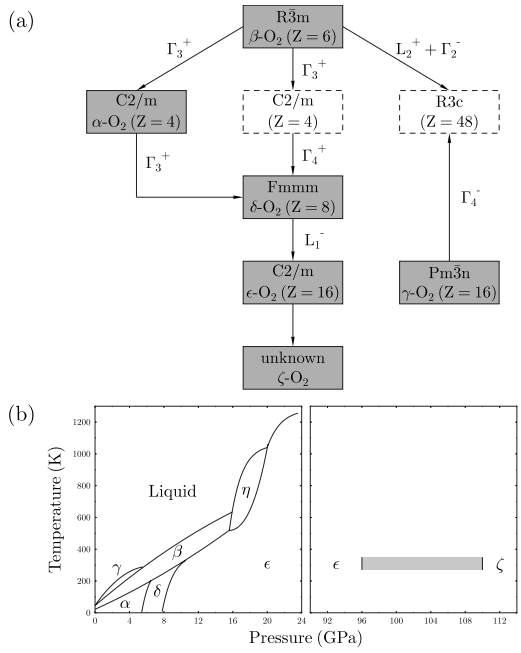

FIG. 1. (a) Symmetry relationship between oxygen phases assumed in our description. White boxes represent hypothetical intermediate phases in the transition mechanisms. The irreducible representations associated with the symmetry-breaking order parameters are indicated along the lines relating the structures, following the notation of Stokes and Hatch (Ref. 11). (b) Temperature-pressure phase diagram of oxygen from Refs. 1, 6, 14, 17, and 20.

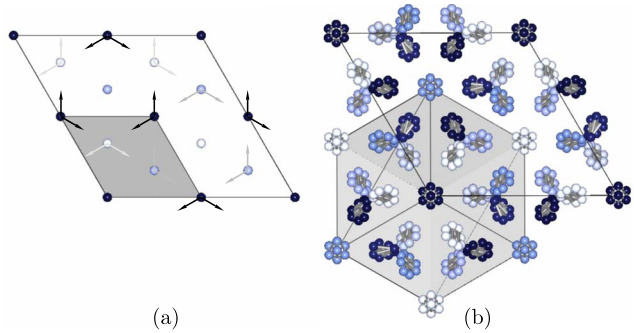

FIG. 2. (Color online) Displacive mechanism associated with the β-$O_2 \rightarrow \gamma$-O_2 phase transition. (a) Trigonal structure of β-O_2 projected along [001]. The β-to-γ phase transition is described as proceeding via a common trigonal substructure ($R3c$, Z=48) with the O_2 centers occupying the Wyckoff position 6a: (0 0 0) in β-O_2 and (0 0 0.0625) in γ-O_2 and 18b: (0 1/2 1/2) in β-O_2 and (1/12 5/12 23/48) in γ-O_2. The arrows indicate displacements of the molecular centers. (b) Cubic structure of γ-O_2 projected along [111]. The cubic unit cell contains eight O_2 molecules centered at the Wyckoff positions 2a and 6c of space group $Pm\bar{3}n$. The molecules centered at the 2a positions are statically disordered with their axes lying with equal probability along one of the four body diagonals. The other six molecules are disordered about the 6c positions. Atoms on different heights along [001] in (a) and [111] in (b) are shown in different gray shades (colors). The trigonal and cubic unit cells of β-O_2 and γ-O_2 are shown as gray polyhedra. The trigonal unit cell of the common $R3c$ substructure is represented by solid lines in (a) and (b).

$\beta \rightarrow \alpha$ transition,[15] in which only the spin-density component M_y and the shear strain e_{xz} have nonzero equilibrium values. It reads as

$$F_1(M_y, e_{xz}) = \frac{a_1}{2}M_y^2 + \frac{b_1}{4}M_y^4 + \frac{b_2}{6}M_y^6 + \frac{c_1}{2}e_{xz}^2 + \frac{c_2}{3}e_{xz}^3 + \frac{c_3}{4}e_{xz}^4 - d_1 M_y^2 e_{xz} - \frac{d_2}{2}M_y^2 e_{xz}^2. \quad (1)$$

Minimizing F_1 with respect to M_y and e_{xz} yield

$$M_y(a_1 + b_1 M_y^2 + b_2 M_y^4 - 2d_1 e_{xz} - d_2 e_{xz}^2) = 0, \quad (2)$$

$$e_{xz}(c_1 + c_2 e_{xz} + c_3 e_{xz}^2 - d_2 M_y^2) - d_1 M_y^2 = 0, \quad (3)$$

which show the following: (1) in the absence of magnetic ordering (M_y=0), a nonzero equilibrium shear strain $e_{xz} = \frac{1}{2c_3}(-c_2 \pm \sqrt{c_2^2 - 4c_1c_3})$ takes place, whereas e_{xz}=0 implies M_y=0. It indicates that in contrast with the current interpretation, the $\beta \rightarrow \alpha$ transition is *structurally driven*, i.e., the *primary* structural mechanism *induces* the onset of the magnetic ordering, imposing a first-order character to the $\beta \rightarrow \alpha$ transition, due to the existence of a cubic invariant e_{xz}^3 in F_1. Therefore, clamping the α phase with the suitable conjugated strain σ_{xz} should cancel the antiferromagnetic order. Let us emphasize that the asymmetry of the free energy F_1 and the resulting quadratic-linear coupling $d_1 M_y^2 e_{xz}$ between the magnetic and structural order parameters are related to the existence in the paramagnetic β-symmetry $R\bar{3}m1'$ of the time-reversal operation which acts on M_y but not on e_{xz}. Such asymmetry was overlooked in previous theoretical studies[12,13] in which the magnetic interactions were expressed, via the Heisenberg Hamiltonian, independently from the interaction potential between O_2 molecules.

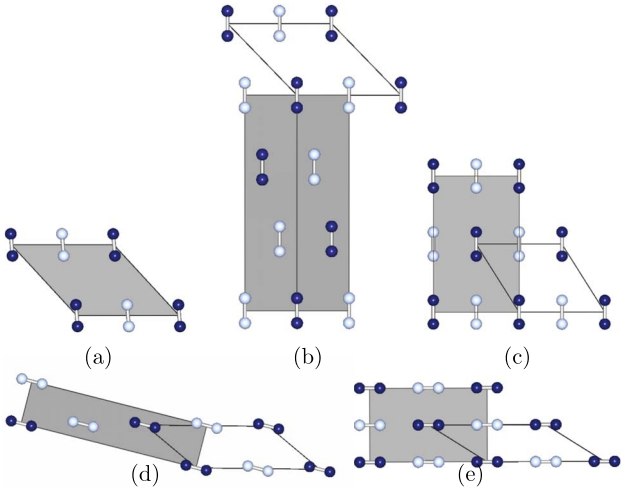

FIG. 3. (Color online) Displacive mechanisms associated with the $\beta \rightarrow \alpha$, $\alpha \rightarrow \delta$, and $\beta \rightarrow \delta$ phase transitions in oxygen. (a) Monoclinic structure of α-O_2 projected along [010]. (b) Trigonal structure of β-O_2 projected along [$1\bar{1}0$]. The β-to-α phase transition is associated with atomic displacements of the order of 0.1 Å within the (a/c) plane with the oxygen atoms occupying the Wyckoff position 4i: (0.1154 0 0.1731) in β-O_2 and (0.0890 0 0.1530) in α-O_2 of the common $C2/m$ unit cell. (c) Orthorhombic structure of δ-O_2 projected along [$0\bar{1}0$]. The α-to-δ phase transition is associated with displacements of the oxygen atoms occupying the Wyckoff position 4i: (0.0890 0 0.1530) in α-O_2 and (0.0871 0 0.1742) in δ-O_2. (d) Trigonal structure of β-O_2 projected along [010]. The β-to-δ transition proceeds via a common monoclinic substructure ($C2/m$, Z=4) with the oxygen atoms occupying the Wyckoff position 4i: (0.0577 0 0.9423) in β-O_2 and (0.0871 0 0) in δ-O_2. (e) Orthorhombic structure of δ-O_2 projected along [010]. The β-to-δ phase transition involves a rotation of the O_2 molecular axes by 13.6°, resulting in a parallel alignment of the molecular axes along the [001] direction in δ-O_2. Atoms on different heights along [010] in (a), [$1\bar{1}0$] in (b), [$0\bar{1}0$] in (c), and [010] in (d), and (e) are shown in different gray shades (colors). The conventional unit cells are shown as gray polyhedra. The unit cells of the common substructures are represented by solid lines.

(2) The phase diagram associated with F_1 (Fig. 4) shows that three phases denoted I to III can be stabilized below the paramagnetic β phase (M_y=0, e_{xz}=0). (i) Two isostructural variants (phases I and II) of the α phase ($M_y \neq 0$, $e_{xz} \neq 0$) displaying the same $C2/m$ structural symmetry and C_p2/m magnetic symmetry. It supports the observation by Jodl *et al.*[16] of an intermediate phase between the α and δ phases, although infrared and x-ray measurements do not confirm this result.[17]

(ii) A nonmagnetic monoclinic structure (M_y=0, $e_{xz} \neq 0$) of symmetry $C2/m$ (phase III), coinciding with the intermediate structure assumed in our proposed $\beta \rightarrow \delta$ transition mechanism, may correspond to the nonmagnetic δ_{II} phase reported by Goncharenko,[6] whereas infrared spectroscopy measurements by Gorelli *et al.*[14] found no evidence of a distinct δ_{II} region.

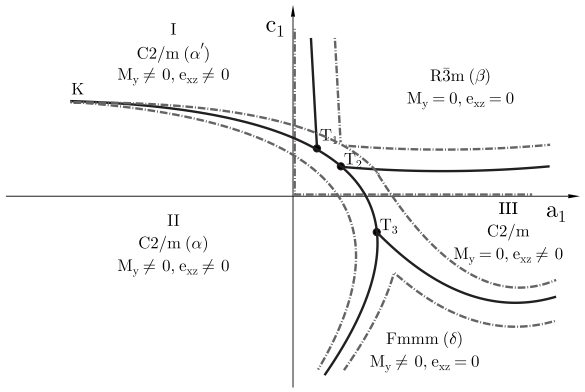

FIG. 4. Theoretical phase diagram associated with the $\beta \rightarrow \alpha$ and $\beta \rightarrow \delta$ transitions in the (c_1, a_1) plane deduced from the minimization of the free energy F_1 given by Eq. (1). Full- and hatched-dotted lines represent, respectively, first-order transition and limit of stability lines. T_1, T_2, and T_3 are triple points. K is a critical point.

(3) Stability of the δ phase requires a shear strain e_{xz} transforming the $C2/m$ symmetry of phase III into $Fmmm$ and triggering an antiferromagnetic order $(M_y \neq 0)$ with magnetic symmetry $Am'mm'$. The triggering mechanism can be foreseen from Eqs. (2) and (3). A nonzero strain $e_{xz} \neq 0$ induces the magnetic component $M_y \neq 0$, which is preserved when e_{xz} vanishes.

The property of the magnetic ordering in oxygen to be structurally driven allows the interpretation of the magnetic collapse occurring at the $\delta \rightarrow \epsilon$ transition. The transition is associated with a four-component order parameter denoted $(\eta_1, \eta_2, \eta_3$, and $\eta_4)$, corresponding to the L_1 instability of the orthorhombic F Brillouin zone. The ϵ structure is stabilized for $\eta_1 = \pm \eta_4$ and $\eta_2 = \eta_3 = 0$. The effective transition free energy is[18]

$$F_2(\eta_1, \eta_4, e_{xz}, L_y) = \frac{\alpha_1}{2}(\eta_1^2 + \eta_4^2) + \frac{\beta_1}{4}(\eta_1^2 + \eta_4^2)^2 + \frac{\beta_2}{4}(\eta_1^4 + \eta_4^4) + \gamma_1(\eta_1^2 + \eta_4^2)e_{xz} + \gamma_2(\eta_1^2 + \eta_4^2)L_y^2 + \frac{1}{2}C_{44}e_{xz}^2 + \frac{\mu}{2}L_y^2. \quad (4)$$

The γ_1 coupling gives rise to an induced shear strain $e_{xz} = -\frac{\gamma_1}{C_{44}}(\eta_1^2 + \eta_4^2)$ in the ϵ phase. The γ_2 term represents the magnetostructural coupling between the displacive order parameter and the induced magnetic ordering. L_y is the projection along y of the antiferromagnetic vector $\mathbf{L} = \mathbf{s}_1 + \mathbf{s}_2 - \mathbf{s}_3 - \mathbf{s}_4$, where the $\mathbf{s}_i$ are atomic spins related by face centering in the δ magnetic structure. Minimizing F_2 with respect to L_y gives $L_y = 0$, i.e., the magnetic ordering cancels in the ϵ phase as the result of the $\delta \rightarrow \epsilon$ structural transition.

Our proposed structural mechanism transforming δ-O_2 into ϵ-O_2 is shown in Fig. 5. It consists of critical displacements by about 0.4 Å, within the (a/c) plane, of oxygen atoms in positions $4i$ in the ϵ structure and of correlated displacements by the same amount of atoms in position $8j$ in general directions. The order-parameter components associated with the displacements read as $[\eta_1(\mathbf{k}_1), \eta_2(\mathbf{k}_2), \eta_3(\mathbf{k}_3), \eta_4(\mathbf{k}_4)]$, where

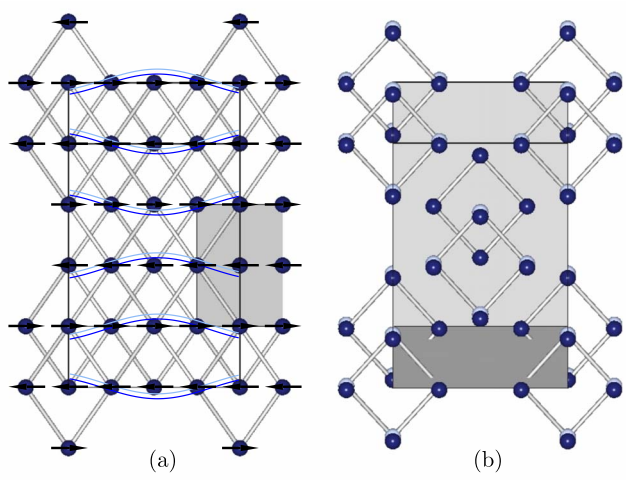

FIG. 5. (Color online) Structural mechanism associated with the δ-$O_2 \rightarrow \epsilon$-O_2 transition. (a) Orthorhombic structure of δ-O_2 projected along the wave vector $\mathbf{k}_1$ corresponding to the direction [001]. The orthorhombic unit cell is shown as a gray polyhedron. The monoclinic unit cell with its origin shifted to $p = (0, 1/2, 0)$ is represented by solid lines. The arrows indicate the directions of the magnetic spins. The δ-to-ϵ phase transition involves periodic displacements of the atoms occupying two Wyckoff positions $4i$: (0.79355 0 0.17420), (0.29355 0 0.17420) in δ-O_2 and (0.82600 0 0.17500), (0.24700 0 0.19200) in ϵ-O_2 and one Wyckoff position $8j$: (0.04355 0.25000 0.17420) in δ-O_2 and (0.03790 0.26660 0.18500) in ϵ-O_2 shown by modulation waves in different colors corresponding to atoms in different heights along [001]. (b) Resulting structure of ϵ-O_2 projected along the wave vector $\mathbf{k}_1$ corresponding to the direction [104]. Atoms on different heights along [001] in (a) and [104] in (b) are shown in different gray shades (colors).

$\mathbf{k}_1 = (-\pi/a, -\pi/b, \pi/c)$, $\mathbf{k}_2 = (\pi/a, \pi/b, \pi/c)$, $\mathbf{k}_3 = (-\pi/a, \pi/b, -\pi/c)$, and $\mathbf{k}_4 = (\pi/a, -\pi/b, -\pi/c)$ represent the four branches of the star of the wave vector corresponding to the L_1 instability. In δ-O_2 $\mathbf{k}_1$, $\mathbf{k}_2$, $\mathbf{k}_3$, and $\mathbf{k}_4$ are perpendicular, respectively, to the (001), (111), (010), and (100) planes, whereas in ϵ-O_2 they are perpendicular to the (001), $(2\bar{2}1)$, (010), and (401) planes. From the calculated displacements occurring at the $\delta \rightarrow \epsilon$ transition given in Fig. 5, one can deduce that the transition mechanism consists of *opposite rotations* by $\pm 2.756°$ of $\mathbf{k}_1$ and $\mathbf{k}_4$ which bring into coincidence the (001) and (100) δ planes onto the (001) and (401) ϵ planes, respectively, the directions of $\mathbf{k}_2$ and $\mathbf{k}_3$ remaining unchanged. Figure 5 shows that the amplitude of the critical displacements is modulated periodically along the [010] δ direction in a way that it lowers the distances between molecules displaying opposite magnetic spins in δ-O_2. The displacement field transforms each two pairs of neighboring molecules in the δ structure into almost regular rhombohedra forming the $(O_2)_4$ clusters in the ϵ structure. The volume drop of about 7%, occurring at the first-order $\delta \rightarrow \epsilon$ transition,[17] coincides with a collapse of the spin-density amplitude and the correlated formation of an equilibrium configuration of $(O_2)_4$ clusters. Our proposed $\delta \rightarrow \epsilon$ transition mechanism reflects at the structural level the underlying changes in the electronic structure leading to the formation

of intermolecular bonding, which have been deduced from inelastic x-ray scattering measurements.[19]

Above 96 GPa, the ϵ structure transforms progressively to a metallic molecular state ζ.[8–10] The transformation proceeds in two stages. (1) An intermediate stage extending from 96 GPa to at least 110 GPa in which one observes a disappearance of the ϵ-O_2 lattice reflections, a continuous evolution of the lattice parameters, and changes in the mosaicity of the crystal.[9] (2) A stabilization of the ζ structure, with a new position of the reflections above a slightly discontinuous transition. The almost continuous character of the transformation is against an interpretation of the intermediate stage as representing an extended region of coexistence between the ϵ and ζ phases.[10] A more likely interpretation is that it constitutes an *intermediate phase* between ϵ-O_2 and ζ-O_2, into which a reorganization of the intermolecular bonding occurs. The indexing of the measured diffraction pattern in the intermediate region with the structural model of the ϵ phase[9] indicates a close relationship between the two phases. Therefore, one can assume that the intermediate phase is either incommensurately modulated or possesses a pseudomonoclinic ϵ structure with a lower triclinic $P\bar{1}$ symmetry giving rise to ferroelastic domains. Along this line, the discontinuous reformation of a single domain crystal above 110 GPa (Ref. 9) reflects the recovery of a higher-symmetry structure.

In summary, the structural phase-transition mechanisms occurring in oxygen have been described and analyzed theoretically. The antiferromagnetic order existing in the α and δ phases has been interpreted as structurally driven. Two isostructural α variants have been suggested to be stable, whereas an intermediate nonmagnetic monoclinic phase was shown to be possibly stable in the $\beta \rightarrow \delta$ transformation process. The magnetic collapse and formation of $(O_2)_4$ clusters observed at the $\delta \rightarrow \epsilon$ transition have been correlated by the same displacement-field mechanism, corresponding to opposite rotations of the (001) and (100) δ-atomic planes. The existence of an intermediate low-symmetry phase is suggested between the ϵ and ζ phases.

ACKNOWLEDGMENT

This work has been supported by the German Science Foundation under Grant No. DE 412/33-1.

*hanne@min.uni-kiel.de

[1] D. A. Young, *Phase Diagrams of the Elements* (University of California Press, Berkeley, 1991).
[2] D. Schiferl *et al.*, Acta Crystallogr., Sect. B: Struct. Sci **39**, 153 (1983).
[3] C. S. Barrett, L. Meyer, and J. Wasserman, J. Chem. Phys. **47**, 592 (1967).
[4] I. N. Goncharenko, O. L. Makarova, and L. Ulivi, Phys. Rev. Lett. **93**, 055502 (2004).
[5] F. A. Gorelli, L. Ulivi, M. Santoro, and R. Bini, Phys. Rev. B **62**, R3604 (2000).
[6] I. N. Goncharenko, Phys. Rev. Lett. **94**, 205701 (2005).
[7] L. F. Lundegaard *et al.*, Nature (London) **443**, 201 (2006).
[8] Y. Akahama, H. Kawamura, D. Hausermann, M. Hanfland, and O. Shimomura, Phys. Rev. Lett. **74**, 4690 (1995).
[9] G. Weck, P. Loubeyre, and R. Le Toullec, Phys. Rev. Lett. **88**, 035504 (2002).
[10] A. F. Goncharov, E. Gregoryanz, R. J. Hemley, and H. K. Mao, Phys. Rev. B **68**, 100102(R) (2003).
[11] H. T. Stokes and D. M. Hatch, *Isotropy Space Groups of the 230 Crystallographic Space Groups* (World Scientific, Singapore, 1988).
[12] P. W. Stephens, R. J. Birgeneau, C. F. Majkrzak, and G. Shirane, Phys. Rev. B **28**, 452 (1983).
[13] R. D. Etters, A. A. Helmy, and K. Kobashi, Phys. Rev. B **28**, 2166 (1983); R. LeSar and R. D. Etters, *ibid.* **37**, 5364 (1988).
[14] F. Gorelli, M. Santoro, R. Bini, and L. Ulivi, Phys. Rev. B **77**, 132103 (2008).
[15] F_1 expresses the coupling between the structural ($R\bar{3}m \rightarrow C2/m$) and magnetic ($R\bar{3}m1' \rightarrow C_p2/m$) orderings occurring at the $\beta \rightarrow \alpha$ transition. The effective form of F_1 is deduced from the order-parameter expansion given in Ref. 11 for the irreducible representation denoted Γ_3^+.
[16] H. J. Jodl, F. Bolduan, and H. D. Hochheimer, Phys. Rev. B **31**, 7376 (1985).
[17] Y. Akahama, H. Kawamura, and O. Shimomura, Phys. Rev. B **64**, 054105 (2001).
[18] The effective form of F_2 is deduced from the four-component order-parameter expansion associated with the irreducible representation L_1^- given in Ref. 11.
[19] Y. Meng *et al.*, Proc. Natl. Acad. Sci. U.S.A. **105**, 11640 (2008).
[20] M. Santoro, E. Gregoryanz, H. K. Mao, and R. J. Hemley, Phys. Rev. Lett. **93**, 265701 (2004).